Available online at www.sciencedirect.com
ScienceDirect
Journal of the European Ceramic Society 28 (2008) 2975–2982
www.elsevier.com/locate/jeurceramsoc

Time-resolved neutron diffraction study of Ti–TiC–Al_2O_3 composites obtained by SHS

M.J. Mas-Guindal [a], X. Turrillas [b], T. Hansen [c], M.A. Rodríguez [a,*]

[a] *Instituto de Cerámica y Vidrio, CSIC, C/Kelsen, N° 5, 28049 Madrid, Spain*
[b] *Eduardo Torroja Institute for Construction Sciences, CSIC, 28033 Madrid, Spain*
[c] *ILL, 6 Rue Jules Horowitz, BP 156, 38042 Grenoble Cedex 9, France*

Received 25 June 2007; received in revised form 26 November 2007; accepted 6 May 2008
Available online 18 June 2008

Abstract

Cermets of the titanium matrix family have potential applications in the aeronautical and automotive fields. Self-propagating high-temperature synthesis (SHS) constitutes a good method to produce them, as it implies low processing costs and energy and time efficiency. An interesting feature of this process is to determine the mechanism of reaction. A good method to do it is the use of *in situ* real-time diffraction techniques. The objective of this paper is to show how the use of time-resolved neutron diffraction (TRND) providing a deeper insight into the mechanism of a typical SHS reaction by monitoring the formation of a cermet of the system Ti–TiC–Al_2O_3. Neutron diffraction experiments have been conducted on Instrument D20 at the Institute Max von Laue-Paul Langevin (Grenoble, France) with a high-flux medium-resolution powder diffractometer. Results show that reaction is initiated with the melting and diffusion of aluminium through the sample, and shortly after product phases are formed. The final product shows a general structure composed of a titanium matrix with the rest of the phases located in reaction domains.

Keywords: Powders-solid state reaction; Composites; Synthesis; Time-resolved neutron diffraction

1. Introduction

Over the last decades, cermets (metal–ceramic composites) have been regarded as advanced engineering materials with very good properties such as low density, excellent oxidation and corrosion resistance, adequate creep resistance at high temperature, good wear resistance and high hardness.[1] A promising cermet family is the one formed by titanium matrix and alumina, which, besides the above-mentioned properties, has the advantage that both, titanium and alumina, have a similar coefficient of thermal expansion, thus resulting in a improved performance when compared with other materials, like SiC-reinforced titanium.[2,3] Most applications arise in the aeronautical and automotive fields. One recent application is in a time-of-flight mass spectrometer of the reflectron type (RTOF), for the study of cometary gases.[4] Less exotic uses have also been found.[5]

One of the problems associated with cermets is the high cost of production, as most traditional techniques, such as slip casting, infiltration or thermal processing require a long time of processing, large amounts of electrical power or heavy equipment, especially when densification is carried out.[6,7] Self-propagating high-temperature synthesis (SHS) constitutes a good alternative method. The main advantages are the low processing costs and energy and time efficiency. It has been used to synthesize a wide variety of materials, such as borides, nitrides, intermetallics, carbides and composites.[8–15] The reaction is usually started by the triggering of a local heating source at the edge of the sample, and the energy released by the reactants makes self-propagation possible through the whole sample. A problem that arises with SHS reactions is that sometimes, the heat released upon combustion is not enough to sustain the propagation of the front, thus making necessary a way for the activation of the reaction; several techniques and variants have been developed with this purpose, like field activated combustion synthesis (FACS), mechanically activated combustion synthesis (MASHS) or chemically activated combustion synthesis. FACS is based on the application of an electrical field of low voltage and high intensity through the sample in order to supply the lack of energy for self-sustenance.[16,17] MASHS is based in the activation of the reactant mixture through energetic milling[18,19]

* Corresponding author. Tel.: +34 91 7355840; fax: +34 91 7355843/45.
E-mail address: mar@icv.csic.es (M.A. Rodríguez).

0955-2219/$ – see front matter © 2008 Elsevier Ltd. All rights reserved.
doi:10.1016/j.jeurceramsoc.2008.05.001

and chemical activation is based in the use of a secondary reaction to supply the necessary energy for the self-sustaining of the reaction.[14,20] Another form of SHS reaction is the thermal explosion (TE) mode, which consists on the global heating of the sample until ignition is produced, normally accompanied with the reaction taking place in the whole sample at the same time; this can also be used as a way for the activation of the reaction.[21,22]

In this paper the reaction involved in the production of titanium-alumina cermets is:

$$3TiO_2 + 4Al \rightarrow 3Ti + 2Al_2O_3 \quad (I)$$

The reaction enthalpy is $\Delta H^\circ = -517\,kJ$, representing a favourable exothermic reaction. The theoretical final product is 41:59 (wt% Ti:Al_2O_3), associated with presence of titanium–aluminium intermetallics.[1,23] The addition of titanium to the reactant mixture results in the production of cermets with enhanced properties, but the reaction enthalpy is decreased, making it necessary to use an activation method. The addition of titanium could be expressed as:

$$xTi + \tfrac{3z}{4}TiO_2 + zAl \rightarrow \tfrac{z}{2}Al_2O_3 + (x + \tfrac{3z}{4})Ti \quad (II)$$

As described elsewhere,[24] a cermet with very good potential properties has a final theoretical relation Ti:Al_2O_3 = 60:40 (wt%). Adjusted reaction is:

$$0.665Ti + 0.585TiO_2 + 0.780Al \rightarrow 1.250Ti + 0.390Al_2O_3 \quad (III)$$

Its enthalpy is 61.395 kJ/mol. The reaction for this stoichiometry is not self-sustained, as mentioned above, so it needs an activation method. The use of a booster (chemical activation) has proven to be a very good option for its production, more precisely the addition of titanium and graphite to the reactants, in order to form TiC, involves a very exothermic reaction that supplies the necessary heat; the process can be optimized by adding a 13% of booster mixture; then the theoretical reaction would be[24]:

$$0.797Ti + 0.510TiO_2 + 0.68Al + 0.218C \rightarrow 1.089Ti + 0.34Al_2O_3 + 0.218TiC \quad (IV)$$

Where part of the Ti reacts with C to supply energy to the system, TiO_2 reacts with Al supplying also energy and also Ti free to the composite.

The main problem to determine the SHS mechanism is the relatively high speed of the reaction. In order to detect the intermediate species (if any), one of the most common methods is the quenching of the reaction to study the phases present at each stage of reaction,[25,26] but it is not always easy to control. A better method is to use *in situ* real-time diffraction techniques, which allow the observation of each stage of the reaction while it is actually occurring. Two of the most used are X-ray and neutron diffraction. Time-resolved X-ray diffraction has been used mainly with high-energy synchrotron radiation with the advantage of getting high-resolution detection[27]; it is mainly used for thin samples or for the surface of big samples.[28,29] Neutrons, on the other hand, can penetrate deeper within the material, thus acquiring data from thicker samples, but more acquisition time is required to obtain a quality as good as with synchrotron radiation. *In situ* time-resolved neutron diffraction (TRND) has been useful, for instance, in monitoring the decomposition of dolomite while heating[30] or studying the mechanism of synthesis of titanium silicon carbide (Ti_3SiC_2)[31] or the kinetics of metal hydride electrodes,[32] as examples.

The objective of this paper is to show how using time-resolved neutron diffraction has allowed us to get a deeper insight on a typical SHS reaction made in explosion mode. Indeed the formation of a titanium-enriched cermet of the system Ti–Al_2O_3 from the initial mixture of Ti, TiO_2, Al and in some cases C (used as a kind of booster), has been examined with a good time resolution according to reactions (III) and (IV). In order to get this, reaction with and without booster has been followed with ultra-high-speed *in situ* neutron diffraction in Instrument D20 at Institute Laue Langevin (Grenoble, France) under the so called thermal explosion mode, which consists in heating the whole sample until the reaction starts through the whole specimen, while recording time-resolved diffraction patterns with a fast acquisition system.

2. Experimental procedure

The raw materials used were: (a) TiO_2-anatase > 99% (Quimialmel, Spain), with particle size $d_{50} = 0.64\,\mu m$ and specific surface, $S_s = 7.7\,m^2/g$; (b) Al-powder > 99% (Alcoa, USA) with $d_{50} = 55\,\mu m$ and $S_s = 0.72\,m^2/g$; (c) Ti > 99% (William Rowland Ltd., UK) with $d_{50} = 96\,\mu m$ and $S_s = 0.03\,m^2/g$; and (d) C-graphite 99.6% (Sofacel, Spain) with $d_{50} = 1.7\,\mu m$ and $S_s = 27\,m^2/g$.

2.1. Preparation of specimens

Powders were weighed according to the stoichiometry of the reactions and attrition milled in a polyethylene attritor mill with zirconia balls (ball-to-powder relation of 2.2 by volume) in isopropyl alcohol (alcohol-to-powder relation of 6.5 by volume) for 40 min. Powder was then dried, compacted and pressed into pellets of 10 g weight with a uniaxial pressure of 7 MPa (30 mm diameter and 5 mm thickness).

In the laboratory experiments were carried out in a polymethylmethacrylate chamber under argon atmosphere. Reaction was ignited passing a AC (20 V) through a tungsten coil.

Measurement of temperature during the process was made by two IMPAC INFRATHERM pyrometers (Germany): one IGA-5 MB18 ranging from 350 to 1800 °C, and one IS-5 MB30 ranging from 1000 to 3000 °C, connected to a computer for data acquisition.

The product obtained was then dried, crushed and ring milled in order to obtain the final powder.

Experiments with TRND were carried out on powders uniaxially pressed into pellets at 7 MPa in a steel die (12 mm diameter and 10 mm high). Five pellets were piled up in the centre of a 16 mm inner diameter silica tube with a wall thickness of 1.5 mm. The tube was placed inside a vertical cylindrical furnace

that works under vacuum with a Niobium cylinder as heating element. The sample was insulated from the base by a small 8-mm-diameter cordierite support; more details can be found in the work of Riley et al.[33]

Neutron diffraction patterns were recorded in transmission mode in Instrument D20 at the Institute Max von Laue-Paul Langevin (Grenoble, France). It is a high-flux (58 MW thermal power) medium-resolution powder diffractometer equipped with a large-area position-sensitive microstrip detector of 1600 cells that allows fast data acquisition in a range between 0 and 160 2θ degrees and in very short time (down to 300 ms).[30,34] A neutron wavelength of 1.3008 Å was selected to cover a total of 1536 points/diffraction pattern.

The specimens were set under vacuum (10^{-3} Pa) and heated up to 400 °C at a linear rate of 10 °C/min while recording a diffraction pattern every 60 s. Then heating at that rate was continued until reaction took place but recording four patterns every second. Then the system was allowed to cool recording also four patterns every second until reaching 400 °C. Under this temperature data acquisition was made at one pattern every 3 s, since no further transformations are observed under this temperature.

2.2. Sample characterization

Bulk and powdered products were embedded in an epoxy resin under vacuum. Polishing was made on a lapping disk with silicon carbide paper down to 2500 grit. The polished surface was then cleaned with isopropyl alcohol, dried and coated by gold sputtering for its examination by FESEM (HITACHI S-4700 microscope, Japan).

2.3. Conventional X-ray diffraction

A Siemens Diffractometer D5000 (Germany) with Cu(Kα) radiation (λ = 1.54056 Å) was used. Data were acquired with 2θ ranging from 20 to 80 °C at a step rate of 0.03° and an acquisition time of 18 s/step. The employed optics were a fixed aperture slit of 2 mm, one scattered-radiation slit of 2 mm after the sample, followed by a system of secondary Soller slits and the reception slit of 0.2 mm. After that, a secondary curved graphite monochromator was placed and finally a detector slit of 0.6 mm.

2.4. Data processing

Visual outlook of phase transformations and the reaction mechanism were obtained using the large array manipulation program Transform.[35]

2.5. Thermodynamic calculations

Calculations were made with the package HSC[36] by Gibbs energy minimization method.

3. Results and discussion

In order to get some idea of the products that could be expected, thermodynamic calculations using HSC software[36] have been made for both compositions: without and with booster. In the case of reaction without booster (Fig. 1a), it is found that during most of the temperature intervals, the expected main phase is TiO, followed by AlTi (most stable between 250 and 1250 °C approximately, and Al_2O_3. In the case of the reaction with booster (Fig. 1b), TiO is the most stable phase in all temperatures, followed by AlTi, TiC and Al_2O_3.

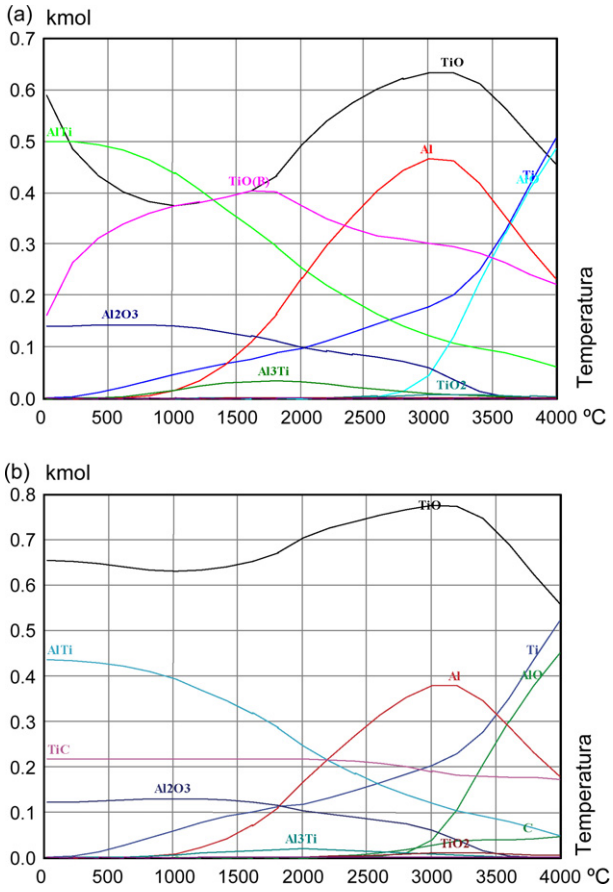

Fig. 1. (a) Thermodynamic products phase prediction for reaction without booster. (b) Thermodynamic products phase prediction for reaction with booster.

3.1. SHS in the laboratory

Pyrometer readings show that the maximum temperature reached is 1950 °C. The temperature profile is shown in Fig. 2. It can be deduced that reaction begins at *ca.* 650 °C, which is close to the melting temperature of aluminium (660 °C), and rises immediately to a maximum during the reaction. Later on, there is a step during which products are synthesized. High temperature is due to the booster effect and the plateau observed at about 1700 °C is probably because of the formation of TiO, as pointed out by Contreras et al.[13] At lower temperatures, the experimental curve is consistent with a cooling model that takes into account both radiation and convection effects.[27] This behaviour leads to suppose that the reaction is accelerated by the melting of aluminium and its diffusion to the whole sample, therefore overcoming the kinetic barrier.

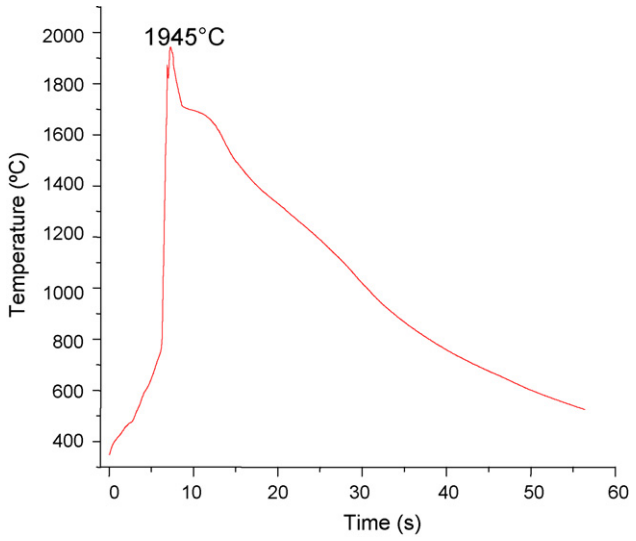

Fig. 2. Temperature plot for reaction with booster measured pyrometrically.

A representative X-ray diffraction pattern is shown in Fig. 3. There is observed the presence of titanium with solid solution of aluminium and oxygen, alumina and titanium carbide with solid solution of oxygen. This solid solution shifts the 2θ position of TiC peaks to a higher angle, than that of pure TiC. A small fraction of high-temperature phase $TiAl_3$ is detected, probably formed due to the high speed of cooling.

3.2. Neutron thermodiffractometry

Experiments were performed under thermal explosion combustion mode, for both compositions, without and with booster. This SHS mode has the main advantage that a heating of the sample until reaction is produced, which ensures, that most of the time, the process will take place. Another advantage of this method is that allows a high reproducibility of the process, since experimental conditions and no uncontrollable variables are involved.

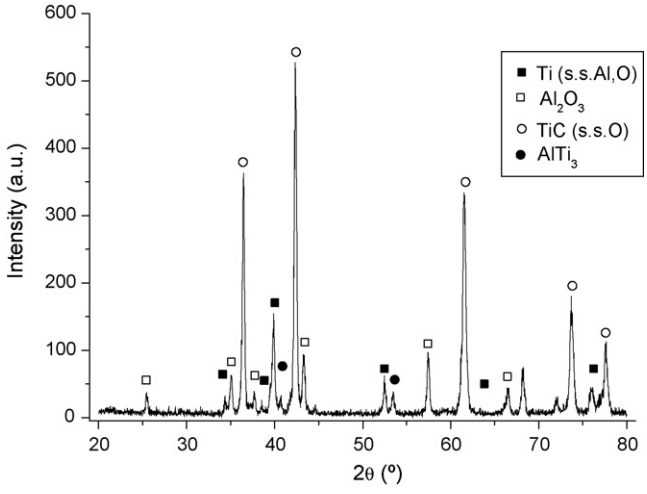

Fig. 3. XRD pattern for product of reaction with booster made at laboratory.

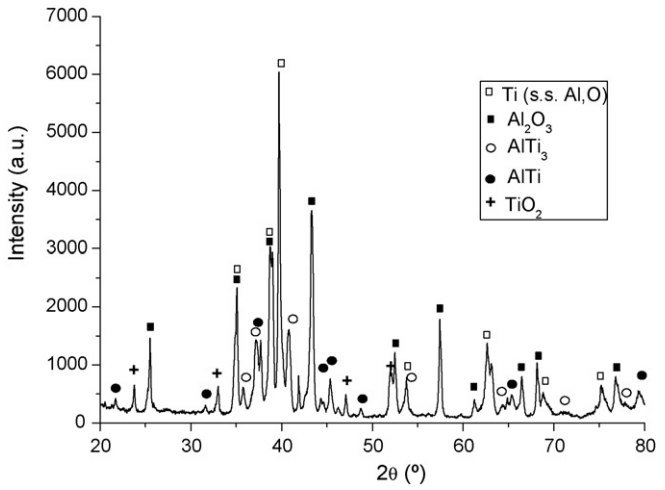

Fig. 4. XRD pattern of product of reaction without booster made by thermal activation.

3.2.1. Thermal explosion without booster

Fig. 4 shows an XRD of the final products which coincide with the phases thermodynamically expected. The main phases are titanium, alumina and two titanium aluminides, Ti_3Al and TiAl. There is also a residue of non-reacted titanium oxide, undetected by neutron diffraction, probably because the reaction has not been completed, and there is some Ti_2O_3 phase (with a similar structure to Al_2O_3). This observation is in agreement with the presence of the Ti_3Al which, according to thermodynamic calculations, is supposed to be present above 1000 °C. So, even under thermal explosion conditions, the reaction to give these cermets is not quantitatively complete.

The use of TRND has allowed understanding of the reaction mechanism. Fig. 5 shows a contour map made with 1000 diffraction patterns collected around the reaction zone and some selected patterns of the main different stages with identified phases spanning along 5 min and a half.

Identified phases correspond to reactants and final products. No intermediate phases have been found. Below 450 °C only peak displacements, due to the thermal expansion, have been observed. For this reason, we will consider this point as the time origin for the plots, in order to enhance the changes produced by the chemical reaction. From this point, observed reaction steps have been:

(a) *Heating*: From start to $t = 166$ s. For the first 166 s the only effect seen is the thermal expansion; *d*-values increase and diffraction angles decrease, see Fig. 5, position A.
(b) *Melting of aluminium*: Melting of aluminium occurs upon heating and it is observed from the disappearance of their corresponding peaks. This starts at $t = 166$ s (position B) and runs for about 10 s (position C), which correspond to a temperature of 650 °C (melting temperature of aluminium is 660 °C).
(c) *Reaction of the sample*: At $t = 200$ s (position D) the diffusion of aluminium through the whole sample triggers the process. The reaction then starts among all reactants at the same time to yield the products. The first phase that is formed

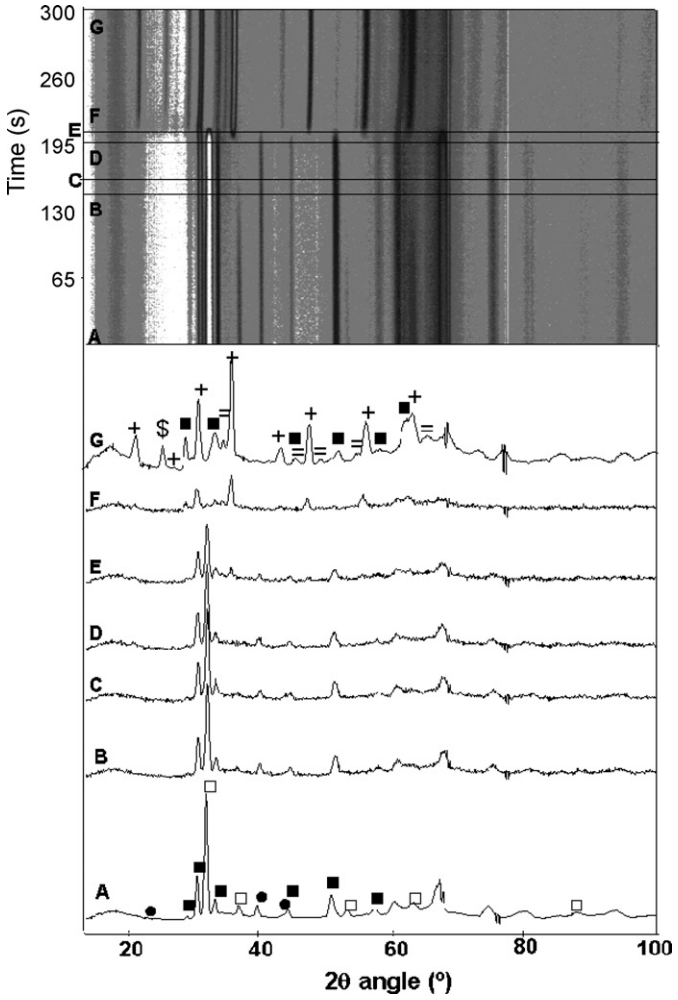

Fig. 5. Contour plot and selected diffractograms corresponding to reaction without booster. Legend for phases is as follows: titanium (■); aluminium (□); anatase (●); alumina (+); titanium aluminide (=); titanium oxide ($).

is the alumina at $t = 206$ s (position E) and the rest of them appear at $t = 216$ s (position F). At this time not any reactants appear. All of them have been consumed or melted, that is in agreement with a synthesis mechanism through precipitation from a liquid.

(d) *Cooling*: Once all the phases have started to form, products consolidate upon cooling until the end of the experiment (position G). No secondary processes are observed through the cooling process.

If reaction zone diffraction patterns are represented in a three-dimensional configuration (Fig. 6), it is observed that peak intensity corresponding to products is lower than that of reactants. This is because metals give a higher diffraction signal.

Fig. 7a shows the SEM general view of the microstructure. It is observed the presence of two zones: one formed of large grains coming from the raw melted titanium, which forms a matrix were alumina zones are embedded; the other zone contains the reacted phases. Upon magnification, as it is observed in Fig. 7b, that reaction zone appears to have a submicronic grain size.

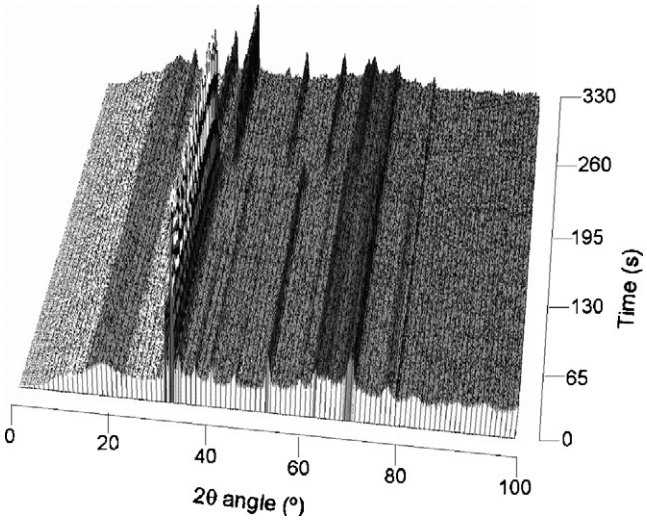

Fig. 6. Three-dimensional map of the reaction without booster.

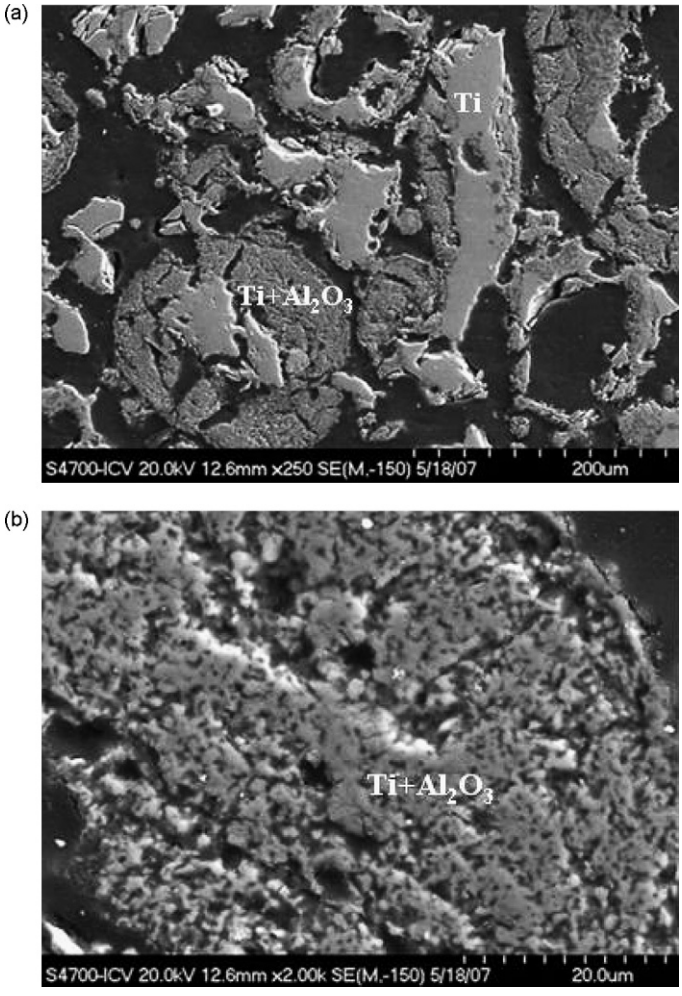

Fig. 7. (a) FESEM general view of product of reaction without booster by thermal activation. (b) FESEM detail view of micronic-sized reacted zone.

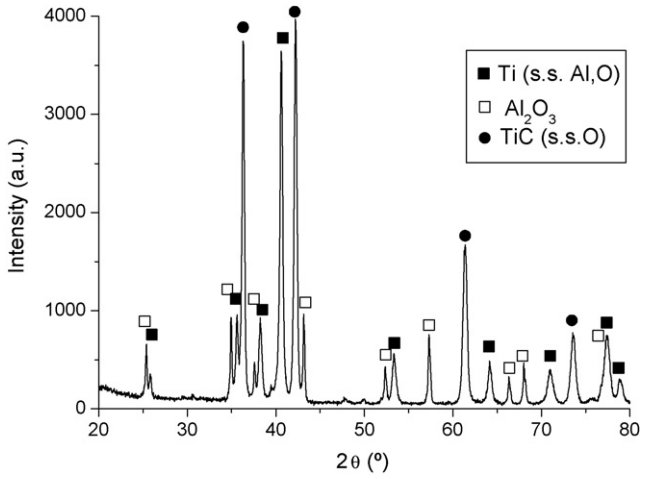

Fig. 8. XRD pattern of product of reaction with booster and thermal activation.

3.2.2. Reaction with booster

The mechanism for reaction (IV) goes in a similar manner as that explained for reaction (III). Products identified are in Fig. 8. It shows titanium with a solid solution of aluminium, alumina and titanium carbide with a solid solution of oxygen. The high-temperature phase Ti_3Al is not formed, but nevertheless the aluminium enters into titanium cells in a similar manner as if forming Ti_3Al; besides, both Ti and Ti_3Al have a similar type of cell (*P*63/*mmc* symmetry); this presence of aluminium atoms also explains the one-2θ-degree displacement of the main reflection of titanium to a higher angle. A similar case happens with the presence of oxygen in the titanium carbide cell, which has been discussed by other authors elsewhere.[24] No AlTi was detected, nor of non-reacted reactants, mainly due to the effect of the booster, as it increases the enthalpy of the reaction and helps to the quantitative formation of the product.

Fig. 9 shows, in a similar way as with non-boostered reactions, a contour map of the process and some diffraction patterns corresponding to the main stages of reaction (labelled A–G), and representing a total time of 6 min and 40 s (400 s). Phases are also only identified in the reactants and products, for no intermediate species are observed. As upon heating until 500 °C nothing special is observed, this point has been considered as starting time. The different stages are:

(a) *Heating*: From start to $t = 50$ s. As it happened in reaction without booster, the only apparent effect is that of the expansion of aluminium and its shift to a higher angle it is represented in position A.
(b) *Melting of aluminium*: At $t = 50$ s (corresponding to a temperature of 600 °C and position B), aluminium starts melting and its peaks disappear at $t = 60$ s (position C). As it melts it starts diffusion through the sample.
(c) *Reaction*: At $t = 144$ s (position D), the diffusion of aluminium makes the whole sample to react at once; the main reaction zone lasts for about 44 s. The first phase to be formed is the one derived from the booster activation, titanium carbide at $t = 150$ s (position E) and it is seen how it consolidates by the progressive shift from a lower angle to the one expected at lower temperature. Probably due to the exothermicity of the TiC formation, the temperature increases at to levels higher than melting point of the raw materials, for this reason not traces of them are observed. The rest of phases form at about $t = 168$ s (position F), after cooling of the system by precipitation. This cooling can be deduced by the evolution of TiC diffraction peaks to smaller 2θ angles (Fig. 9). Considering temperature profile (Fig. 2), this precipitation begins at 1700 °C.
(d) *Cooling*: At $t = 188$ s (position G), the reaction and precipitation is already finished and the cooling continues without any other transformation. The final products correspond to position H and have been recorded every minute in order to detect the less diffracting phases.

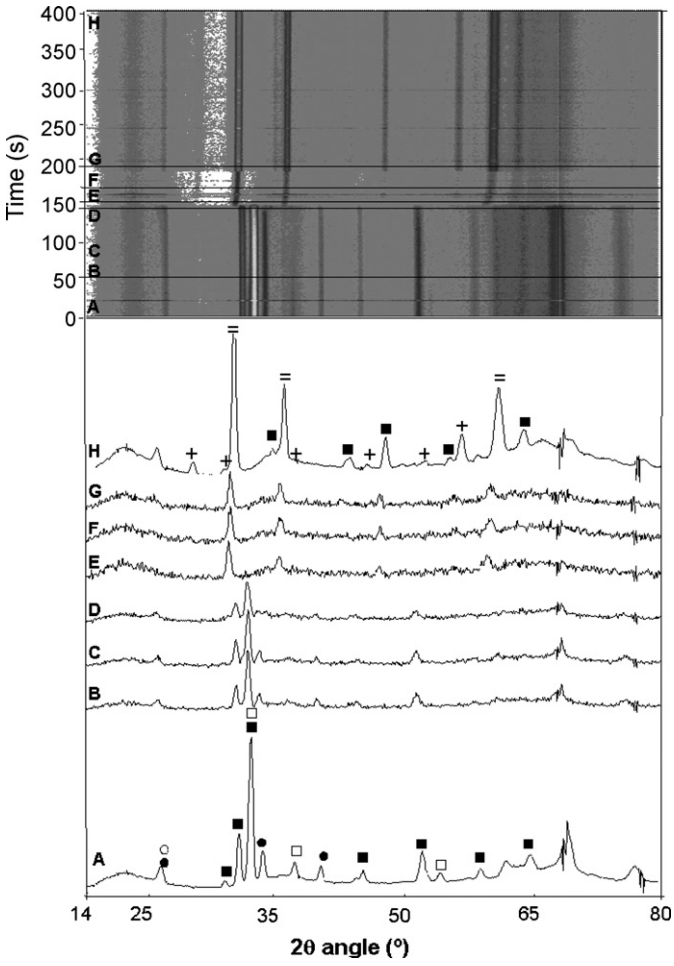

Fig. 9. Contour plot and selected diffractograms corresponding to reaction with booster and thermal activation. Legend for phases is as follows: titanium (■); aluminium (□); anatase (●); graphite (◯); alumina (+); titanium carbide (=).

If a three-dimensional representation of the reaction zone is made (Fig. 10) it is observed also the difference of diffraction level of metal reactants and ceramics. It is also observed the evolution of peaks at the reaction zone.

Fig. 11a shows a general SEM view of the microstructure. It is appreciated the presence of two main zones, as happened with the composition without booster. Large zones correspond to the titanium phase. The effect of the additional heating provided by

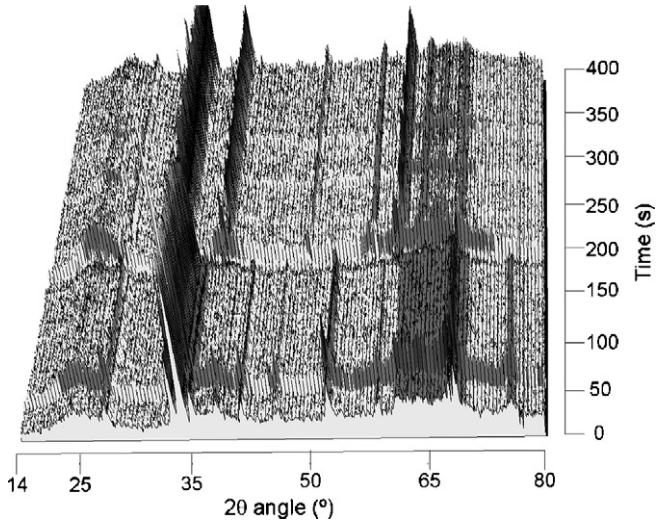

Fig. 10. Three-dimensional map of the reaction with booster.

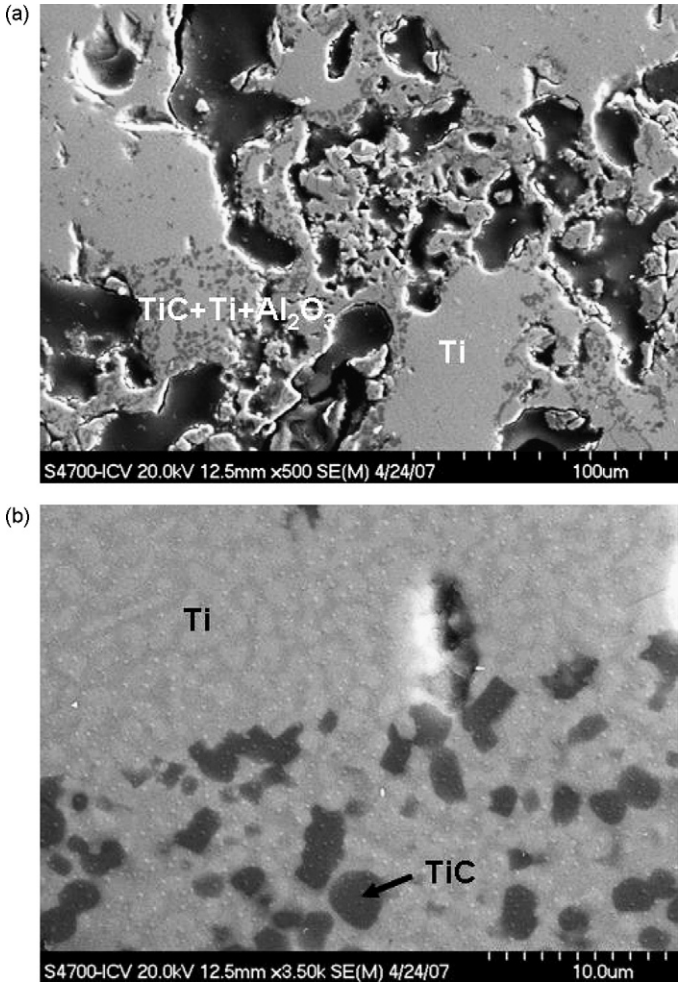

Fig. 11. (a) FESEM general view of product of reaction with booster and thermal activation. (b) FESEM detail view of product with booster and thermal activation, showing phase distribution.

the booster can be appreciated in the fact that these grains are almost forming a continuous matrix through the whole sample. The other zone is formed of micron-sized grains. A magnification of large grains, Fig. 11b, shows that within the grains there are different micron-size phases distributed heterogeneously: dark ones correspond mainly to alumina and the lighter ones to titanium phases either titanium or titanium carbide.

4. Conclusions

Thermal explosion provides a way of activating SHS reactions with low enthalpy; however, combining this technique with Time Resolved Diffractometry, provides a very good tool for *in situ* monitoring of reactions, and to tackle their mechanisms.

This is the case of the combustion reaction to produce titanium-enriched cermets in the system Ti–Al_2O_3. The increased amount of reactant titanium makes reaction to be non-self-sustained, and activation by means of a booster or thermal explosion, is needed.

By conducting the reactions at ILL Neutron Diffractometry Facilities, in a reactor equipped with a heating element, it has been possible to follow the evolution of reaction at real time, as well as providing a way for the activation of the sample.

This evolution has shown that reaction starts with the melting and diffusion of aluminium to the whole of the sample, and then it proceeds very quickly to form the products.

In the case of reaction without booster, it is first observed the formation of aluminium oxide phase, the melting of all reactants, and then the precipitation of the rest of them.

In the case of reaction with booster first phase to be formed is titanium carbide, the exothermicity of this process, increase a lot the temperature of the system and it remain liquid during more than 40 s of cooling. After that, precipitation of the rest of phases takes place.

Thanks to the study in real time it can be stated that reaction takes place from the liquid. Is mainly a precipitation from melted raw materials. No other kind of mechanisms as solid–liquid or dissolution precipitation occurs.

Obtained material is very heterogeneous, mainly due to the big differences among reactants particle size. This heterogeneity can be overcome during processing (milling) of composite before shape forming and sintering.

Acknowledgements

Authors wish to thank ILL, for beamtime granted through experiments 5-25-133 and 5-25-134. This work has been supported by the European Project NAMAMET (STREP NMP3-CT-2004-0014TO) and co-financed by the Spanish Science and Technology Agency (CICYT) under Project No. MAT2004-04923-C02-01.

References

1. Fan, R., Liu, B., Zhang, J., Bi, J. and Yin, Y., Kinetic evaluation of combustion synthesis $3TiO_2 + 7Al \rightarrow 3TiAl + 2Al_2O_3$ using non-isothermal DSC method. *Mater. Chem. Phys.*, 1995, **91**, 140–145.

2. Kelkar, G. P. and Carim, A. H., Phase equilibria in the Ti–Al–O system at 945 °C and analysis of Ti/Al_2O_3 reactions. *J. Am. Ceram. Soc.*, 1997, **78**, 572–576.
3. Misra, A. K., Reaction of Ti and Ti–Al alloys with alumina. *Met. Mater. Sci.*, 1991, **22A**, 715–721.
4. Zigerlig, B., Elsener, H. R., Piazza, D. and Kisser, M., Brazing, welding and design aspects of a multifunctional titanium–alumina ceramic composite component for a space application. In *Proceedings of the 6th International Conference on Joining Ceramics Glass and Metal*, 2002, pp. 66–73.
5. Matsunaga, K., Nakamura, A., Yamamoto, T. and Ikuhara, Y., Theoretical study of defect structures in pure and titanium-doped alumina. *Solid State Ion.*, 2004, **172**, 155–158.
6. Tomoshige, R., Goto, T., Matsushita, T., Imamura, K., Chiba, A. and Fujita, M., High-temperature-shock compaction of ceramics/silicide composites produced by combustion synthesis. *J. Mater. Process. Technol.*, 1999, **85**, 100–104.
7. Welham, N. J., Willis, P. E. and Kerr, T., Mechanochemical formation of metal–ceramic composites. *J. Am. Ceram. Soc.*, 2000, **83**, 33–40.
8. Munir, Z. A. and Anselmi-Tamburini, U., Self-propagating exothermic reactions: the synthesis of high-temperature materials by combustion. *Mater. Sci. Rep.*, 1989, **7–8**, 277–365.
9. Merzhanov, A. G., History and recent developments in SHS. *Ceram. Int.*, 1995, **21**, 371–379.
10. Patil, K. C., Aruna, S. T. and Mimani, T., Combustion synthesis: an update. *Curr. Opin. Solid State Mater. Sci.*, 2002, **6**, 507–512.
11. Curfs, C., Cano, I. G., Vaughan, G. B. M., Turrillas, X., Kvick, Å. and Rodríguez, M. A., TiC–NiAl composites obtained by SHS: a time-resolved XRD study. *J. Eur. Ceram. Soc.*, 2002, **22**, 1039–1044.
12. Cano, I. G., Borovinskaya, I. P., Rodriguez, M. A. and Grachev, V. V., Effect of dilution and porosity on self-propagating high-temperature synthesis of silicon nitride. *J. Am. Ceram. Soc.*, 2002, **85**, 2209–2211.
13. Contreras, L., Turrillas, X., Mas-Guindal, M. J., Vaughan, G. B. M., Kvick, Å. and Rodríguez, M. A., Synchrotron diffraction studies of TiC/FeTi cermets obtained by SHS. *J. Solid State Chem.*, 2005, **178**, 1595–1600.
14. Mas-Guindal, M. J., Contreras, L., Turrillas, X., Vaughan, G. B. M., Kvick, Å. and Rodríguez, M. A., Self-propagating high-temperature synthesis of TiC–WC composite materials. *J. Alloy. Compd.*, 2006, **419**, 227–233.
15. Moya, J. S., Iglesias, J. E., Limpo, J., Makhonin, N. S. and Rodríguez, M. A., Single crystal AlN fibers obtained by self-propagating high-temperature synthesis (SHS). *Acta Mater.*, 1997, **45**, 3089–3094.
16. Munir, Z. A. R., Lai, W., and Ewald, K. H., Field-assisted combustion synthesis, Unites States Patent 5380409 (10 January 1995).
17. Feng, A., Graeve, O. A. and Munir, Z. A., Modeling solution for electric field-activated combustion synthesis. *Comput. Mater. Sci.*, 1998, **12**, 137–155.
18. Uenishi, K., Matsubara, T., Kambara, M. and Kobayashi, K. F., Nanostructured titanium-aluminides and their composites formed by combustion synthesis of mechanically alloyed powders. *Scr. Mater.*, 2001, **44**, 2093–2097.
19. Suryanarayana, C., Mechanical alloying and milling. *Prog. Mater. Sci.*, 2001, **46**, 1–184.
20. Licheri, R., Orrù, R. and Cao, G., Chemically-activated combustion synthesis of TiC–Ti composites. *Mater. Sci. Eng. A—Struct. Mater. Prop. Microstruct. Process.*, 2004, **367**, 185–197.
21. Horvitz, D., Gotman, I., Gutmanas, E. Y. and Claussen, N., In situ processing of dense Al_2O_3–Ti aluminide interpenetrating phase composites. *J. Eur. Ceram. Soc.*, 2002, **22**, 947–954.
22. Biswas, A., Porous NiTi by thermal explosion mode of SHS: processing, mechanism and generation of single phase microstructure. *Acta Mater.*, 2005, **53**, 1415–1425.
23. Welham, N. J., Mechanical activation of the solid-state reaction between Al and TiO_2. *Mater. Sci. Eng. A—Struct. Mater. Prop. Microstruct. Process.*, 1998, **255**, 81–89.
24. Mas-Guindal, M. J., Benko, E. and Rodríguez, M. A., Nanostructured metastable cermets of Ti–Al_2O_3 through activated SHS reaction. *J. Alloy. Compd.*, 2008, **454**, 352–358.
25. Jiang, G., Zhuang, H. and Li, W., Mechanistic investigation of the field-activated combustion synthesis of tungsten carbide with or without cobalt added. *Combust. Flame*, 2003, **135**, 113–121.
26. Xiao, G., Fan, Q., Gu, M. and Jin, Z., Microstructural evolution during the combustion synthesis of TiC–Al cermet with larger metallic particles. *Mater. Sci. Eng. A—Struct. Mater. Prop. Microstruct. Process.*, 2006, **425**, 318–325.
27. Contreras, L., Turrillas, X., Vaughan, G. B. M., Kvick, Å. and Rodríguez, M. A., Time-resolved XRD study of TiC–TiB2 composites obtained by SHS. *Acta Mater.*, 2004, **52**, 4783–4790.
28. Gras, C., Bernsten, N., Bernard, F. and Gaffet, E., The mechanically activated combustion reaction in the Fe—Si system: in situ time-resolved synchrotron investigations. *Intermetallics*, 2002, **10**, 271–282.
29. Sharafutdinov, M. R., Korchagin, M. A., Shkodich, N. F., Tolochko, B. P., Tsygankov, P. A. and Yagubova, I. Y., Phases transformations in the Ni–Al system investigation by synchrotron radiation diffraction. *Nucl. Instrum. Methods Phys. Res. Sect. A—Accel. Spectrom. Dect. Assoc. Equip.*, 2007, **575**, 149–151.
30. De Aza, A. H., Rodríguez, M. A., Rodríguez, J. L., De Aza, S., Pena, P., Convert, P. *et al.*, Decomposition of dolomite monitored by neutron thermodiffractometry. *J. Am. Ceram. Soc.*, 2002, **85**, 881–888.
31. Kisi, E. H., Riley, D. P. and Curfs, C. C., Ultra-high speed neutron diffraction studies of combustion synthesis. *Physica B*, 2006, **385–386**, 487–492.
32. Latroche, M., Chabre, Y., Decamps, B., Percheron-Guégan, A. and Noreus, D., In situ neutron diffraction study of the kinetics of metallic hydride electrodes. *J. Alloy Compd.*, 2002, **334**, 267–276.
33. Riley, D. P., Kisi, E. H., Hansen, T. C. and Hewat, A. W., Self-propagating high-temperature synthesis of Ti_3SiC_2: I, ultra-high-speed neutron diffraction study of the reaction mechanism. *J. Am. Ceram. Soc.*, 2002, **85**, 2417–2424.
34. http://whisky.ill.fr/YellowBook/D20/.
35. Research Systems Inc. (Kodak Company), Sterling, VA, 20164, USA. Program NOeSYS, Version 1.2, 1998. Available from: www.rsinc.com.
36. Roine, A., HSC CHEMISTRY 5.11 ©Outokumpu Research Oy, Pori, Finland, http://www.outokumpu.com/hsc.